Chapter 3

Design of PSS and TCSC Using Genetic Algorithm

3.1 Introduction

This chapter deals with the individual and simultaneous application of thyristor controlled series capacitor and power system stabilizer for dynamic power system stability improvement. The Genetic Algorithm based Controllers have been designed for the development of the control strategy for thyristor control series capacitor and power system stabilizer. The parameters tuning of genetic algorithm based PSS and TCSC are considered as an optimization problem and the parameters are tuned using genetic search algorithm under different operating points. The non-linear and linerizied model of the synchronous machine which includes both the generator main field winding and the damper winding on q-axis has been considered for the effective analysis of the system. The non-linear simulation of single machine infinite bus has been carried out, results of which show the efficacy and capability of simultaneous application both controllers under the various operating conditions and disturbances. The results demonstrate the improvement in the dynamic performance of the system with proposed control algorithms. The time response analysis have been performed under different operating conditions and contingencies.

3.2 GA based Design of CPSS and PID-PSS

3.2.1 Genetic Algorithm

Genetic Algorithms (GAs) are adaptive heuristic search algorithms introduced on the evolutionary themes of natural selection. The fundamental concept of the GA design is to model processes in a natural system that is required for evolution, specifically those that follow the principles posed by Charles Darwin to find the survival of the fittest. GAs constitute an intelligent development of a random search within a defined search space to solve a problem. GA was first pioneered by John Holland in the 1960s, and has been widely studied, experimented, and applied in numerous engineering disciplines. GA has been used for optimizing the parameters of the control system that are complex and difficult to solve by conventional optimization methods. GA maintains a set of candidate solutions called population and repeatedly modifies them. At each step, the GA selects individuals from the current population to be parents and uses them to produce the children for the next generation. Candidate solutions are usually represented as strings of fixed length, called chromosomes. A fitness or objective function is used to reflect the goodness of each member of the population. Given a random initial population, GA operates in cycles called generations, as follows [8]:

- Each member of the population is evaluated using a fitness function.
- The population undergoes reproduction in a number of iterations. One or more parents are chosen stochastically, but strings with higher fitness values have higher probability of contributing an offspring.
- Genetic operators, such as crossover and mutation, are applied to parents to produce offspring.
- The offspring are inserted into the population and the process is repeated.

Some of the advantages of GAs are as follows [90]:

1. GA is capable of parallel processing.

2. A large solution set can be obtained very quickly by GA.

3. GA is well suitable for complex, non linear and noisy fitness function.

4. GA is capable of converging to the local minima.

3.2.2 Problem Formulation and Optimization Function

Here, different parameters of the conventional PSS (Equ.2.78) and PID-PSS (Equ.2.85) are optimized under different operating conditions. For the conventional power system stabilizer the time constants T_1,T_2,T_3,T_4, and the gain K_{pss} are optimized using real coded genetic search algorithm. For the Proportional Integral Derivative - PSS, the gain K_p,K_I and K_D are optimized using real coded GA. In the both type of PSS input feedback signal is rotor speed, and under the steady state operation, the output of the PSS is zero. Under the disturbance conditions, the output of PSS is modified according to the change in the speed during dynamic environment. In this study, objective is to minimize the optimization function, which is described by equation (3.1).

$$J = \int_0^T t\,|\triangle\omega_m(t)|\,dt \tag{3.1}$$

The optimization function has been developed such that the damping factor of the system be improved and minimize real part of the eigen values associated with the rotor mode. The minimization of eigen values show that closed loop poles of the systems are located very far away in s-plane from origin. Hence time response parameters such as settling time to be improved and overshoots to be reduced. The Time Multiplied by Absolute Error (ITAE) [65, 97] has been used as the performance index. The optimization function J follows the optimized performance of CPSS and PID-PSS controlled system, and CPSS and PID-PSS gains for the system are adjusted such that the performance index to be minimized. The performance index is calculated over a time interval T, normally in the region of $(0 \leq t \leq T)$, where t is the settling time of the system. The best system response is obtained when the both PSS parameters are optimized by minimizing the maximum eigen values over a certain

range of operating conditions. The optimization flow chart of GA based CPSS and PID-PSS is shown in Figure 3.1.

Optimized J subject to:

For conventional Power system stabilizer

$$T_1^{min} \leq T_1 \leq T_1^{max} \tag{3.2}$$

$$T_2^{min} \leq T_2 \leq T_2^{max} \tag{3.3}$$

$$T_3^{min} \leq T_3 \leq T_3^{max} \tag{3.4}$$

$$T_4^{min} \leq T_4 \leq T_4^{max} \tag{3.5}$$

$$K_{pss}^{min} \leq K_{pss} \leq K_{pss}^{max} \tag{3.6}$$

For Proportional Integral Derivative - Power system stabilizer

$$K_p^{min} \leq K_P \leq K_p^{max} \tag{3.7}$$

$$K_I^{min} \leq K_I \leq K_I^{max} \tag{3.8}$$

$$K_D^{min} \leq K_D \leq K_D^{max} \tag{3.9}$$

3.2.3 Calculation of Initial Conditions

The initial conditions of the synchronous machine are calculated for different operating conditions. Four operating conditions are considered such as normal loading, slight heavy loading, heavy loading and very heavy loading. Here active power $P_t = 0.6, 0.75, 0.9, 0.12$ and reactive power $Q_t = 0.0224, 0.1, 0.15, 0.2$ are considered as different loading conditions. The initial conditions of different variables described by section (2.3.1) are calculated. The initial conditions of $i_{d0}, i_{q0}, v_{d0}, v_{q0}, E'_{q0}, E'_d, \delta_0$ are given in Table 3.1. By using these values, K_1 (Equ.2.68) to K_{10} (Equ. 2.77) constants of the machine are calculated. Then after the

eigen values, damping factor, right eigen vector, left eigen vector and participation factors (Section:2.4.3) of the machine have been calculated under four different operating conditions. Table 3.2 represents values of machine constant at different loading conditions.

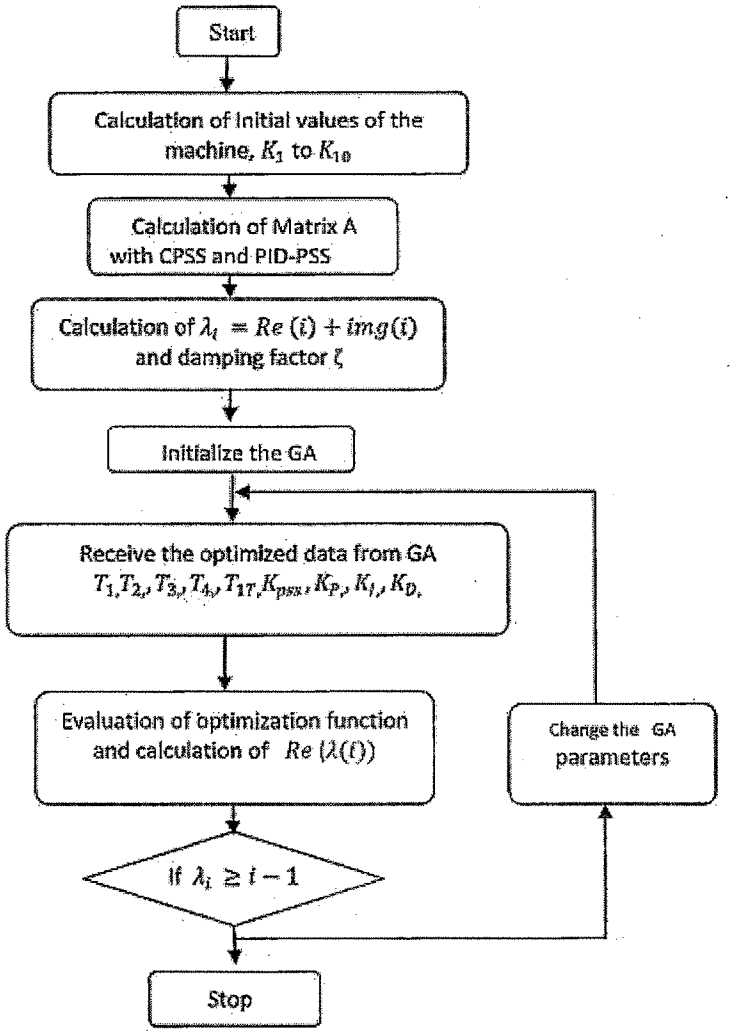

Figure 3.1: Flow Chart of GA based PSSs

Table 3.1: Calculation of Initial Conditions

Sr.No	Operating conditions	i_{d0}	i_{q0}	v_{d0}	v_{q0}	E'_{d0}	E'_{q0}	δ_0
1	$P_t = 0.6, Q_t = 0.0224$	-0.383	0.425	-0.674	0.806	-0.232	0.969	61.52
2	$P_t = 0.75, Q_t = 0.1$	-0.553	0.455	-0.72	0.764	-0.248	1.0015	64.95
3	$P_t = 0.9, Q_t = 0.15$	-0.724	0.489	-0.765	0.7191	-0.2763	1.025	68.42
4	$P_t = 1.2, Q_t = 0.2$	-1.03	0.531	-0.841	0.628	-0.289	1.065	74.9

Table 3.2: Value of K_1 to K_{10} Constant

Operating Conditions	K_1	K_2	K_3	K_4	K_5
$P_t = 0.6, Q_t = 0.0224$	0.726523	1.434816	0.317627	0.452937	1.061707
$P_t = 0.75, Q_t = 0.1$	0.764320	1.514948	0.223680	0.452937	1.094229
$P_t = 0.9, Q_t = 0.15$	0.786620	1.587298	0.132994	0.452937	1.123214
$P_t = 1.2, Q_t = 0.2$	0.796368	1.709019	-0.041301	0.452937	1.166157

Contd...

K_6	K_7	K_8	K_9	K_{10}
0.759433	-0.151024	-0.074594	0.472187	-0.253221
0.759433	-0.134110	-0.077964	0.447764	-0.270886
0.759433	-0.116467	-0.082909	0.421359	-0.287812
0.759433	-0.082475	-0.095970	0.368063	-0.316500

3.2.4 Eigen values and Participation Factor

The linear model of the system has been considered and eigen values of the Matrix A is calculated with both types of the PSSs under the different operating conditions. The matrix A of the different state space models described by equations (2.67), (2.84) and (2.86) are used for calculation of eigen values and eigen vectors. For the effective operation of the PSSs, the participation factor methods [4, 15] are used for identification of the eigen values associated with electromechanical modes. The magnitude of the participation factors are calculated using right eigen vector and left eigen vector.

3.2.5 Results

The linearized model presented by Figures 2.3 and 2.6 have been used for the small signal stability analysis of the SMIB system without PSS and with PSS respectively. For different operating conditions, the oscillations of the electromechanical modes of the machine are identified with GA based CPSS and PID-PSS, and small signal stability of the system has been analyzed.

The initial conditions, eigen values, damping factors and participation factors of the system are calculated using MATLAB programming. For four operating conditions, the objective function described by equations (3.2) to (3.9) are optimized. The time domain simulation is performed and fitness value is determined through equation (3.1) for each set of the gain and time constant parameters of CPSS and PID-PSS. By changing the GA parameters such as population size, crossover rate and function, mutation rate and function, number of generation, etc, the new set of gains and time constants are developed and best fitness values are selected. The parameters are selected for expected solution is given by Table 3.3 for the normal operating condition. The appropriate choice of the GAs parameters affects the convergence rare of the algorithm. Figure 3.2 shows the relationship between numbers of population versus convergence of fitness function under normal operating conditions. The optimized parameters of CPSS and PID-PSS are tuned for expected solution which is given by Table 3.4 and Table 3.5 respectively. All eigen values and corresponding damping factor without PSS and with GA based PSSs are shown in Table 3.10. The magnitude of participation factor of CPSS under the different operating conditions are shown in Table 3.6 to 3.9.

Table 3.3: GA Parameters and Values

GA Parameters	Values/function
Population size	50
Stopping Generation	65
Scaling function	rank
Selection function	Stochastic Uniform
Mutation function	Gaussian
Crossover function	Scattered

Table 3.4: Optimized Parameters of CPSS

Parameters	Operating Points			
	1	2	3	4
K_{pss}	4.562	4.691	4.962	5.232
T_1	0.97	1.089	1.83	2.11
T_2	0.994	0.849	2.419	2.821
T_3	0.633	0.362	0.432	0.523
T_4	0.0161	0.078	0.173	0.213

Table 3.5: Optimized Parameters of PID-PSS

Parameters	Operating Points			
	1	2	3	4
K_P	0.0256	0.0255	0.315	0.385
K_I	0.269	0.256	0.328	0.415
K_D	11.618	12.618	13.75	14.21

Table 3.6: Participation Factor (first operating condition)-CPSS

$P_t = 0.6, Q_t = 0.0224$							
0.0008	0.0039	0.0039	**0.5173**	**0.5173**	0.0051	0.0011	0.0269
0.0008	0.0039	0.0039	**0.5173**	**0.5173**	0.0051	0.0006	0.0269
0.1149	0.4974	0.4974	0.0298	0.0298	0.0000	0.0000	0.0056
0.0000	0.0000	0.0000	0.0398	0.0398	0.0000	0.0001	1.0630
0.2264	0.4174	0.4174	0.0031	0.0031	0.0000	0.0000	0.0004
0.0018	0.0061	0.0061	0.0654	0.0654	1.0105	0.0245	0.0058
0.0011	0.0038	0.0038	0.0401	0.0401	0.0002	1.0232	0.0083
0.6632	0.0405	0.0405	0.0211	0.0211	0.0000	0.0000	0.0004

Table 3.7: Participation Factor (second operating condition)-CPSS

$P_t = 0.75, Q_t = 0.1$							
0.0140	0.0140	0.0252	**0.5442**	**0.5442**	0.0054	0.0158	0.0157
0.0140	0.0140	0.0252	**0.5442**	**0.5442**	0.0054	0.0152	0.0157
0.6246	0.6246	0.1815	0.0424	0.0424	0.0000	0.0006	0.0073
0.0003	0.0003	0.0004	0.0386	0.0386	0.0000	0.0024	1.0545
0.4557	0.4557	0.4789	0.0050	0.0050	0.0000	0.0000	0.0005
0.0079	0.0079	0.0129	0.0582	0.0582	1.0111	0.0509	0.0004
0.0158	0.0158	0.0279	0.1133	0.1133	0.0003	1.0859	0.0305
0.2996	0.0761	0.0758	0.1345	0.1345	0.0000	0.0016	0.0002

Table 3.8: Participation Factor (third operating condition)-CPSS

$P_t = 0.9, Q_t = 0.15$							
0.0222	0.0222	0.2844	**0.6563**	**0.6563**	0.0066	0.0128	0.0159
0.0222	0.0222	0.2844	**0.6563**	**0.6563**	0.0066	0.0077	0.0159
0.8205	0.8205	0.2024	0.0847	0.0847	0.0000	0.0001	0.0068
0.0006	0.0006	0.0251	0.0336	0.0336	0.0000	0.0002	1.0475
0.7098	0.7098	0.0544	0.0128	0.0128	0.0000	0.0000	0.0005
0.0029	0.0029	0.0367	0.0285	0.0285	1.0151	0.0334	0.0007
0.0128	0.0128	0.2076	0.1263	0.1263	0.0018	1.0172	0.0183
0.1997	0.0450	0.0222	0.3545	0.3545	0.0001	1.0172	0.0183

Table 3.9: Participation Factor(Fourth operating condition)-CPSS

$P_t = 1.2, Q_t = 0.2$							
0.0523	0.0523	**0.8220**	**0.8220**	0.6051	0.0074	0.0219	0.0158
0.0523	0.0523	**0.8220**	**0.8220**	0.6051	0.0074	0.0078	0.0158
1.0148	1.0148	0.1705	0.1705	0.3595	0.0000	0.0001	0.0054
0.0011	0.0011	0.0344	0.0344	0.0500	0.0000	0.0001	1.0575
0.8070	0.8070	0.0289	0.0289	0.0865	0.0000	0.0000	0.0004
0.0050	0.0050	0.0385	0.0385	0.0603	1.0174	0.0336	0.0014
0.0219	0.0219	0.1725	0.1725	0.3222	0.0025	1.0171	0.0169
0.3668	0.0399	0.0068	0.7198	2.9158	0.0002	0.0006	0.0128

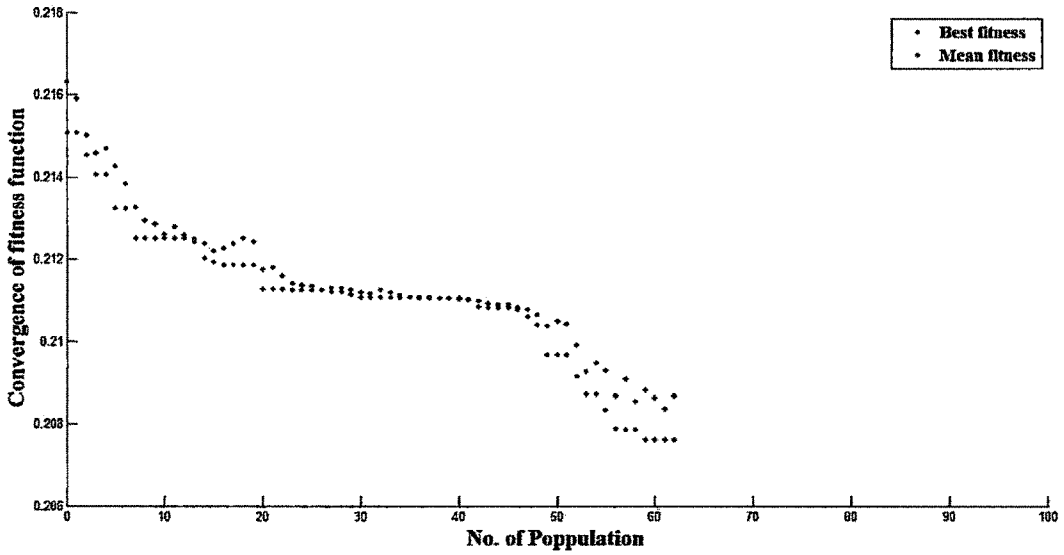

Figure 3.2: Numbers of population versus convergence of fitness function with PSS at Normal operating condition

Attention to Table 3.10, for all operating conditions, without application of PSS second pair of eigen value is positive and damping factor corresponding to same eigen value is negative. The positive eigen values show instability of system. While using of CPSS and PID-PSS, all the eigen values are negative with positive damping factor. This shows that system has become stable using power system stabilizer.

The eigen values associated to the only electromechanical mode (rotor mode) is evaluated using participation factor for all operating points. Attention to Table 3.10, the eigen values

associated with rotor mode are positive with negative damping factor without PSS. The damping factor are -0.0002, -0.0094, -0.0196,-0.0451 for four operating conditions. The oscillatory frequency of rotor mode is increased which shows instability of the system.

With CPSS, for first operating condition to third operating condition, the λ_4 and λ_5 have significant participation in rotor mode and for fourth operating condition, $\lambda 3$ and $\lambda 4$ have higher participation in rotor mode. eigen values and corresponding participation factor have been shown by bold font in Table 3.10, and Table 3.6 to 3.9 respectively. The damping factors associated to rotor mode are 0.1786, 0.2920, 0.3071, 0.4155 for all operating conditions using CPSS. Using right and left eigen vectors, the participation factors are calculated for PID-PSS.

With PID-PSS, second pair of eigen values (i.e. λ_3 and λ_4) have significant participation in rotor mode for all operating conditions. The bold font in Table 3.10 represents the eigen values and the damping factors 0.4483, 0.4109, 0.5726, 0.7484 associated to rotor mode for all operating conditions.

The CPSS and PID-PSS significantly improved the eigen values, damping factor and reduced oscillatory frequency in rotor mode. The eigen values of system have shown that the location of closed loop poles are in the left half of the s-pane and results show that the system has become stable using by CPSS and PID-PSS. Hence stability of power system has been improved using PSSs under different loading conditions.

Table 3.10: Eigen values and Damping Factor of CPSS and PID-PSS

O.C.	without PSS		With PSS			
			CPSS		PID-PSS	
	eigen value	ξ	eigen value	ξ	eigen value	ζ
1	-20.3431 +27.1736i	0.5993	-80.8871	1.0000	-17.1033 +24.9993i	0.5647
	-20.3431 -27.1736i	0.5993	-10.1653 +42.3526i	0.2334	-17.1033 -24.9993i	0.5647
	0.0012 + 6.4014i	-0.0002	-10.1653 -42.3526i	0.2334	**-3.3149 + 6.6100i**	**0.4483**
	0.0012 - 6.4014i	-0.0002	**-0.7752 + 4.2697i**	**0.1786**	**-3.3149 - 6.6100i**	**0.4483**
	-2.6404	1.0000	**-0.7752 - 4.2697i**	**0.1786**	-2.4857	1.0000
			-2.6678	1.0000	-0.0021	1.0000
			-0.1005	1.0000		
			-1.0054	1.0000		
2	-20.3826 +26.0738i	0.6159	-10.7327 +27.2905i	0.3660	-17.4124 +25.1619i	0.5690
	-20.3826 -26.0738i	0.6159	-10.7327 -27.2905i	0.3660	-17.4124 -25.1619i	0.5690
	0.0623 + 6.6531i	-0.0094	-29.0967	1.0000	**-2.9977 + 6.6512i**	**0.4109**
	0.0623 - 6.6531i	-0.0094	**-1.4417 + 4.7212i**	**0.2920**	**-2.9977 - 6.6512i**	**0.4109**
	-2.6836	1.0000	**-1.4417 - 4.7212i**	**0.2920**	-2.5007	1.0000
			-2.6813	1.0000	-0.0031	1.0000
			-1.1954	1.0000		
			-0.1005	1.0000		
3	-20.4367 +24.8339i	0.6354	-16.8994 +22.3471i	0.6032	-15.4249 +21.4022i	0.5847
	-20.4367 -24.8339i	0.6354	-16.8994 -22.3471i	0.6032	-15.4249 -21.4022i	0.5847
	0.1348 + 6.8749i	-0.0196	-8.6414	1.0000	**-4.9546 + 7.0932i**	**0.5726**
	0.1348 - 6.8749i	-0.0196	**-1.9660 + 6.0933i**	**0.3071**	**-4.9546 - 7.0932i**	**0.5726**
	-2.7204	1.0000	**-1.9660 - 6.0933i**	**0.3071**	-2.5610	1.0000
			-2.7348	1.0000	-0.0040	1.0000
			-0.4103	1.0000		
			-0.1007	1.0000		
4	-20.5971 +22.1444i	0.6811	-15.8036 +18.9297i	0.6409	-12.1260 +16.7328i	0.5868
	-20.5971 -22.1444i	0.6811	-15.8036 -18.9297i	0.6409	-12.1260 -16.7328i	0.5868
	0.3284 + 7.2704i	-0.0451	**-2.8438 + 6.2254i**	**0.4155**	**-8.2177 + 7.2835i**	**0.7484**
	0.3284 - 7.2704i	-0.0451	**-2.8438 - 6.2254i**	**0.4155**	**-8.2177 - 7.2835i**	**0.7484**
	-2.7868	1.0000	-7.9133	1.0000	-2.6315	1.0000
			-2.8131	1.0000	-0.0053	1.0000
			-0.1007	1.0000		
			-0.3518	1.0000		

3.3 GA based Design of TCSC and PSS

3.3.1 Problem Formulation and Optimization Function

Different parameters of the PSS and TCSC are optimized using real coded genetic algorithm under four operating conditions. For the conventional power system stabilizer, the time constants T_1,T_2,T_3,T_4, and the gain K_{pss} are optimized. For the TCSC controller the time constant T_{1T},T_{2T},, T_{3T},, T_{4T}, and K_C are tuned using real coded genetic search algorithm. For PSS and TCSC, the time constant of wash out filter T_w and T_{w1} has been selected to be 10. The rotor speed signal has been utilized as feedback signal for both the stabilizer. Here, it is objective to minimize the optimization function J. The optimization flow chart has been shown in Figure (3.3). The optimization function is described by equation (3.10).

$$J = \int_0^T t\,|\triangle\omega_m(t)|\,dt \tag{3.10}$$

The optimization function has been developed such that the damping factor of the system be improved by minimization of real part of the eigen values associated with the rotor mode. Hence time response parameters such as settling time is to be improved and overshoots is to be reduced. The Time Multiplied by Absolute Error (ITAE) has been used as the performance index. The optimization function J follows the optimized performance of PSS and TCSC controlled system. The CPSS and TCSC gains for the system are adjusted such that the performance index to be minimized. The performance index is calculated over a time interval T, normally in the region of $(0 \leq t \leq T)$, where t is the settling time of the system. The best system response is obtained when the PSS and TCSC parameters are optimized by minimizing the maximum eigen values over a certain range of operating conditions. The flow chart 3.3 shows the optimization of PSS and TCSC parameters. Optimize J subject to:

$$T_1^{min} \leq T_1 \leq T_1^{max} \tag{3.11}$$

$$T_2^{min} \leq T_2 \leq T_2^{max} \tag{3.12}$$

$$T_3^{min} \leq T_3 \leq T_3^{max} \tag{3.13}$$

$$T_4^{min} \leq T_4 \leq T_{14}^{max} \tag{3.14}$$

$$T_{1T}^{min} \leq T_{1T} \leq T_{1T}^{max} \tag{3.15}$$

$$T_{2T}^{min} \leq T_{2T} \leq T_{2T}^{max} \tag{3.16}$$

$$T_{3T}^{min} \leq T_{3T} \leq T_{4T}^{max} \tag{3.17}$$

$$T_{4T}^{min} \leq T_{4T} \leq T_{4T}^{max} \tag{3.18}$$

$$K_{pss}^{min} \leq K_{pss} \leq K_{pss}^{max} \tag{3.19}$$

$$K_C^{min} \leq K_C \leq K_C^{max} \tag{3.20}$$

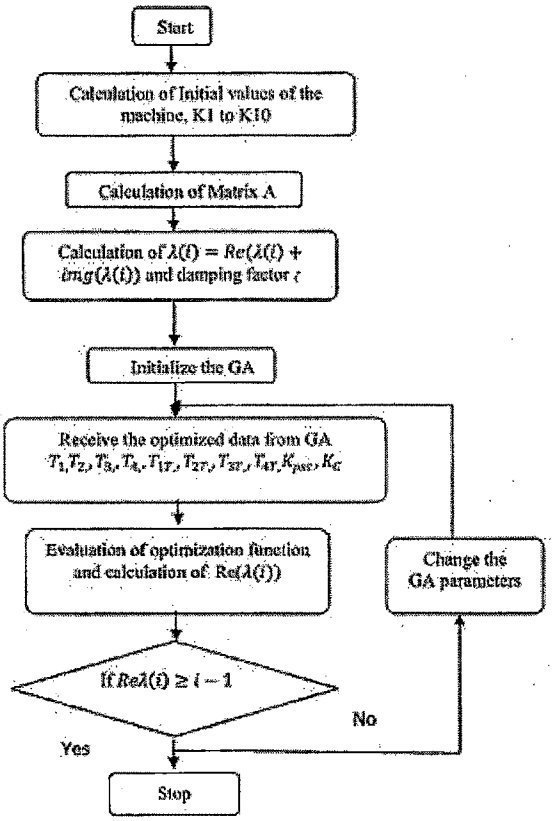

Figure 3.3: Flow chart of GA based PSS and TCSC

3.3.2 Calculation of $K_1$to K_{10} Constants

The initial conditions of the synchronous machine are calculated for different operating conditions. Four operating conditions are considered such as light loading, normal loading and heavy loading and very heavy loading. Here active power $P_t = 0.6, 0.75, 0.9, 1.2$ and reactive power $Q_t = 0.0224, 0.1, 0.15, 0.2$ are used as different loading conditions. The initial conditions of different variables described by section (2.3.1) are calculated. The initial conditions of $i_{d0}, i_{q0}, v_{d0}, v_{q0}, E'_{q0}, E'_d, \delta_0$ are given in Table 3.1. After addition of TCSC, new values of K_1 to K_{10} constants (Table: 3.11) are calculated using initial conditions. The constant of the machine are changed as line reactance of the system would be changed after changing of line reactance X_e to X_{net}. Then after the eigen values, damping factor, right eigen vector, left eigen vector and participation factors (Section: 2.4.3) of the machine are calculated under the four different operating conditions.

Table 3.11: Values of K_1 to K_{10}Constant after inclusion of TCSC

Operating Conditions	K_1	K_2	K_3	K_4	K_5
$P_t = 0.6, Q_t = 0.0224$	0.800705	1.533198	0.371039	0.424146	1.193447
$P_t = 0.75, Q_t = 0.1$	0.843310	1.618670	0.283385	0.424146	1.230004
$P_t = 0.9, Q_t = 0.15$	0.869186	1.695800	0.198232	0.424146	1.262585
$P_t = 1.2, Q_t = 0.2$	0.882877	1.825553	0.034083	0.424146	1.310857

Contd...

K_6	K_7	K_8	K_9	K_{10}
0.745751	-0.162542	-0.092693	0.435552	-0.223638
0.745751	-0.144338	-0.096039	0.413023	-0.239239
0.745751	-0.125349	-0.100948	0.388668	-0.254187
0.745751	-0.088765	-0.113915	0.339507	-0.279524

3.3.3 Eigen values and Participation factor

The linear model of the system has been considered and eigen values of the state matrix A are calculated with individual application of TCSC, and simultaneously design of PSS and TCSC under the different operating conditions. The matrix A of the different state space models described by equations (2.91) and (2.92) are used for calculation of eigen values and

eigen vectors. For the effective operation of the PSS, the participation factor [4, 15] methods are used for identification of the eigen values associated with electromechanical modes. The magnitude of the participation factors are calculated using right eigen vector and left eigen vector.

3.3.4 Results

The linearized model presented by Figure 2.12 has been used for the small signal stability analysis of the SMIB system with TCSC and PSS. For different operating conditions, the oscillations of the electromechanical modes of the machine are identified with GA based CPSS and TCSC, and small signal stability of the system is analyzed.

The initial conditions, eigen values, damping factors and participation factors of the system are calculated using MATLAB programming. For four operating conditions, the objective function described by equation (3.11) to (3.20) have been optimized. The time domain simulation is performed and fitness value is determined through equation (3.10) for each set of the gain and time constant parameters of CPSS and TCSC. By changing the GA parameters such as population size, crossover rate and function, mutation rate and function, number of generation, etc, the new set of gains and time constants are developed and best fitness values have been selected. The GA parameters are selected for expected solution and are given by Table 3.3 for the normal operating condition. The appropriate choice of the GAs parameters affects the convergence rare of the algorithm. The relationship between numbers of population versus convergence of fitness function of TCSC and PSS-TCSC under normal operating conditions has been shown by Figures 3.4 and 3.5 respectively. The optimized parameters of CPSS and TCSC are tuned for expected solution which is given by Table 3.12. All eigen values and damping factor with individual application of TCSC and simultaneous application of PSS and TCSC is shown in Table 3.13 .

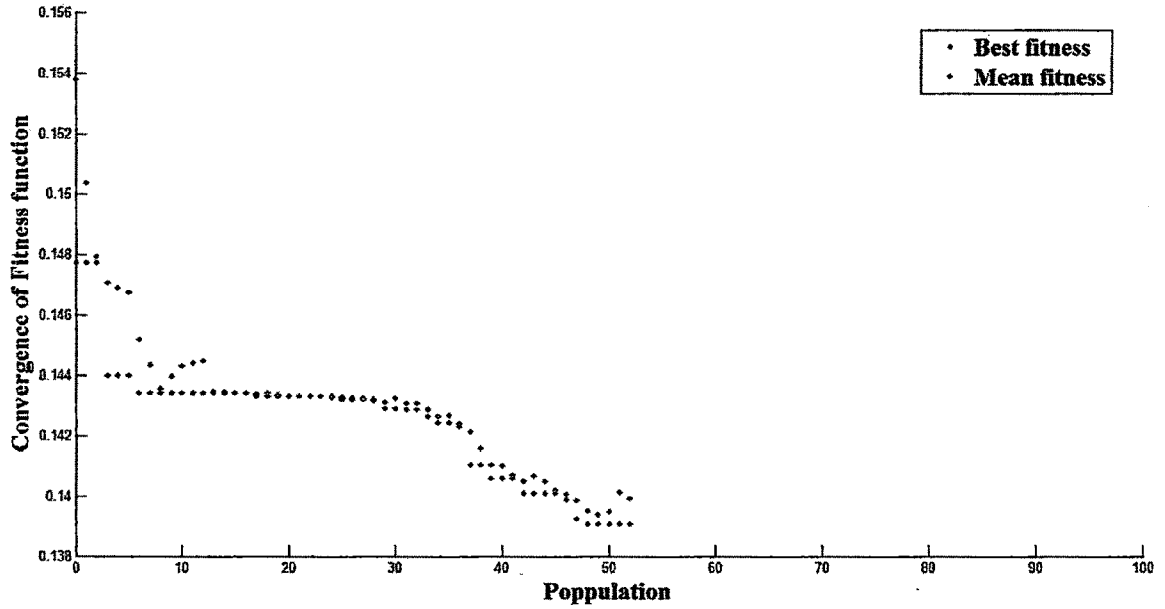

Figure 3.4: Numbers of population versus convergence of Fitness Function with TCSC at Normal Operating Condition

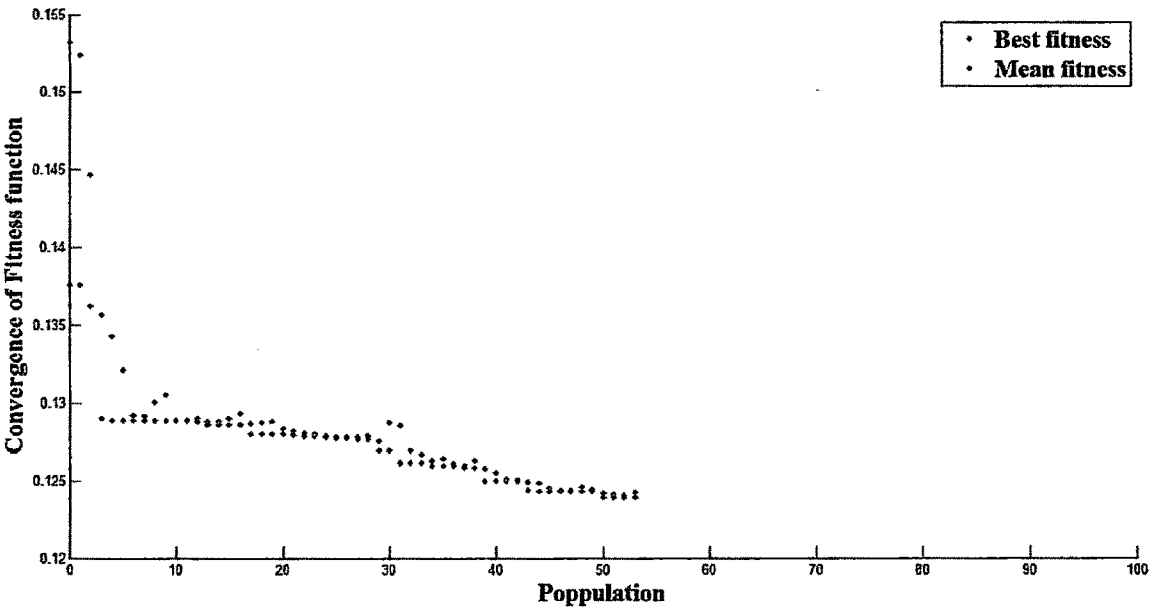

Figure 3.5: Numbers of population versus convergence of Fitness Function with PSS and TCSC at Normal Operating Condition

Table 3.12: Optimized Parameter of TCSC and PSS

Parameter	Operating Conditions			
	1	2	3	4
K_C	50.253	70.256	85.256	95.256
T_{1T}	0.1382	0.1464	0.1589	0.1682
T_{2T}	0.1091	0.1402	0.1358	2.1423
T_{3T}	0.1135	0.1235	0.1125	0.1323
T_{4T}	0.1645	0.1524	0.1687	2.1789
K_{pss}	4.562	4.691	4.962	5.232
T_1	0.97	1.089	1.83	2.111
T_2	0.994	0.849	2.419	2.821
T_3	0.633	0.362	0.432	0.523
T_4	0.0161	0.078	0.173	0.213

Table 3.13: Eigen values and Damping factor of PSS and TCSC

O.C.	TCSC		PSS and TCSC	
1	eigen values	ζ	eigen values	ζ
	-68.6920	1.0000	-84.2000	1.0000
	-16.9056 +15.2140i	0.7433	-66.3827	1.0000
	-16.9056 -15.2140i	0.7433	-7.4441 +39.2017i	0.1866
	-2.7191 + 9.8082i	**0.2671**	-7.4441 -39.2017i	0.1866
	-2.7191 - 9.8082i	**0.2671**	-9.2578	1.0000
	-9.4529	1.0000	**-2.1424 + 4.2892i**	**0.4469**
	-4.9141	1.0000	**-2.1424 - 4.2892i**	**0.4469**
	-3.0040	1.0000	-5.4183	1.0000
	-0.1008	1.0000	-3.0116	1.0000
			-0.9809	1.0000
			-0.1068	1.0000
			-0.0000	1.0000
2	-71.3735	1.0000	-71.7830	1.0000
	-17.8289 +12.4113i	0.8207	-36.0467	1.0000
	-17.8289 -12.4113i	0.8207	-3.1731 +23.4427i	0.1341
	-0.6254 +10.5403i	**0.0592**	-3.1731 -23.4427i	0.1341
	-0.6254 -10.5403i	**0.0592**	**-3.0735 + 4.2816i**	**0.5832**
	-0.1003	1.0000	**-3.0735 - 4.2816i**	**0.5832**
	-3.3571	1.0000	-5.9775	1.0000
	-5.1883	1.0000	-6.9985	1.0000
	-6.9348	1.0000	-3.3244	1.0000
			-1.1287	1.0000
			-0.1088	1.0000
			0.0000	-1.0000

Table 3.14: Eigen values and Damping factor of PSS and TCSC....Contd...

3	-73.7957	1.0000	-73.9565	1.0000
	-18.9081 +13.5580i	0.8127	-20.7877	1.0000
	-18.9081 -13.5580i	0.8127	-1.9973 +12.6794i	0.1556
	1.9050 + 9.1233i	**-0.2044**	-1.9973 -12.6794i	0.1556
	1.9050 - 9.1233i	**-0.2044**	**-6.0822 + 4.1356i**	**0.8269**
	-0.0995	1.0000	**-6.0822 - 4.1356i**	**0.8269**
	-3.6162	1.0000	-8.8109	1.0000
	-5.0999	1.0000	-3.4876	1.0000
	-6.8422	1.0000	-5.9690	1.0000
			-0.3711	1.0000
			-0.1116	1.0000
			-0.0000	1.0000
4	-66.7339	1.0000	-66.7363	1.0000
	-20.8003 +20.5770i	0.7109	-14.5965 +16.0765i	0.6722
	-20.8003 -20.5770i	0.7109	-14.5965 -16.0765i	0.6722
	0.5379 + 7.8571i	**-0.0683**	**-3.7172 + 6.8400i**	**0.4775**
	0.5379 - 7.8571i	**-0.0683**	**-3.7172 - 6.8400i**	**0.4775**
	-2.8547	1.0000	-8.5977	1.0000
	-0.4421 + 0.1715i	0.9323	-2.8793	1.0000
	-0.4421 - 0.1715i	0.9323	-0.4277 + 0.1625i	0.9348
	-0.0962	1.0000	-0.4277 - 0.1625i	0.9348
			-0.3381	1.0000
			-0.1090	1.0000
			-0.0000	1.0000

The participation factor method is used for identification of eigen values and damping factor associated to electromechanical mode using TCSC and PSS-TCSC. Attention to Table 3.13, for all operating conditions, the damping factor of system has been improved with application of TCSC and PSS-TCSC. The eigen values and damping factors related to rotor mode shown by bold font in Table 3.13. With TCSC, for the two operating conditions the eigen values associated with rotor mode is negative and damping factor is positive. For remaining last two operating conditions, the eigen values associated with rotor mode is positive and damping factor are negative. With TCSC, the damping factor associated to rotor mode are 0.2671, 0.0592, -0.2044,-0.0683 for four operating conditions, while with simultaneous application of PSS and TCSC, damping factors associated to rotor mode are 0.4469, 0.5832, 0.8269, 0.4775 for four operating conditions. The application of PSS-TCSC,

significantly improved the eigen values, damping factors and reduced oscillatory frequency in rotor mode. The simultaneous application of PSS and TCSC have provided good stability to the system as eigen values and damping factors are improved compare to individual application of PSS and TCSC. The closed poles are very far away in the left half of the s-pane using PSS-TCSC compare to individual damping controller.

3.4 Non-linear Simulation

The nonlinear model of the power system has been used for the transient stability analysis of the SMIB system with generator attached PSS and transmission line connected TCSC. The initial conditions of the different variables are calculated using MATLAB programming. The non-linear simulation is carried out using non-linear dynamic model described by equations (2.6) to (2.11), which has been implemented using MATLAB/simulink environment. The detailed data of the power system used in this study is given by Appendix A. Comparison analysis between CPSS and PID-PSS, and individual and simultaneous application of TCSC and CPSS are carried out under different operating conditions, faults and disturbance. These disturbances are considered such as the three phase short circuit at sending end and middle of transmission line, outage of transmission line, suddenly changes in mechanical input and step changes in terminal voltage reference.

For case 1 to case 6, the time response of rotor speed deviation ω_m(rad/sec), rotor angle δ (degree), terminal voltage V_t (p.u.) and net line reactance X_{net} (p.u.) have been shown in figures. Without application of controllers, oscillations in rotor speed deviation have been observed, which shows the marginal stability and instability of the system. While PSS and TCSC have provided damping to the synchronous machine and have improved the power system stability. With application of damping controllers, the system becomes stable and different time response parameters have been improved.

3.4.1 Case I

Considering operating condition 1 as defined in table 3.1 $P_t = 0.6, Q_t = 0.0224$. A three phase fault is created at 1s at the sending end of one the circuits of the transmission line and cleared after 100ms [33]. The original system restored after the fault clearance. The response of the rotor speed deviation between 0s to 10s with damping coefficient $D = 0$ and without PSS and TCSC damping controllers has been shown in Figure 3.6. Figures 3.7, 3.8 and 3.9 have shown the response of speed deviation between 0s to 30s, 30s to 60s and 60s to 90s respectively with zero damping coefficient and without damping controllers. The transient response during faulted condition between 1s to 2s has been shown in Figure 3.10. The response of the δ and ω_m with presence of GA based CPSS and PID-PSS have been shown in Figure 3.11 and 3.12 respectively. The response of ω_m and X_{net} with individual and simultaneously application of GA based TCSC and PSS have been shown in Figure 3.13 and 3.14 respectively. Figures 3.6, 3.7, 3.8 and 3.9 have shown that the oscillations in rotor speed deviation are growing. While using individual PSSs and TCSC and simultaneous application of GA based PSS-TCSC significantly diminished this oscillation in the system and provided very good damping characteristics.

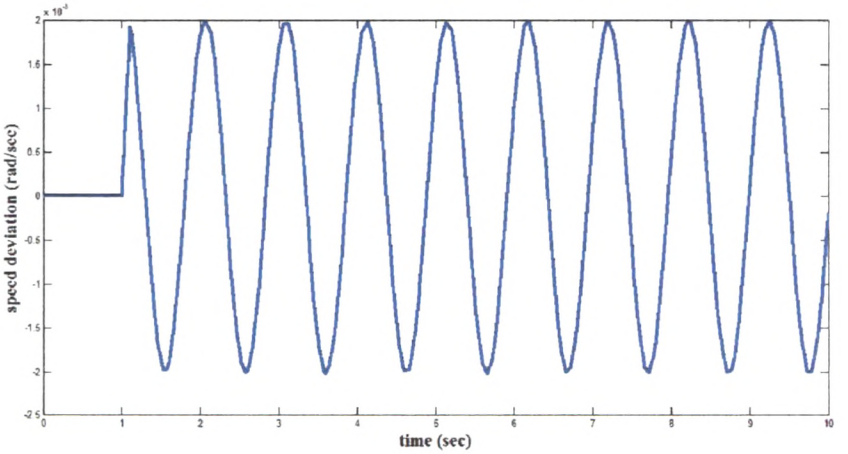

Figure 3.6: Case I: Speed deviation between 0s to 10s with damping coefficient $D = 0$ and without controller (PSS and TCSC)

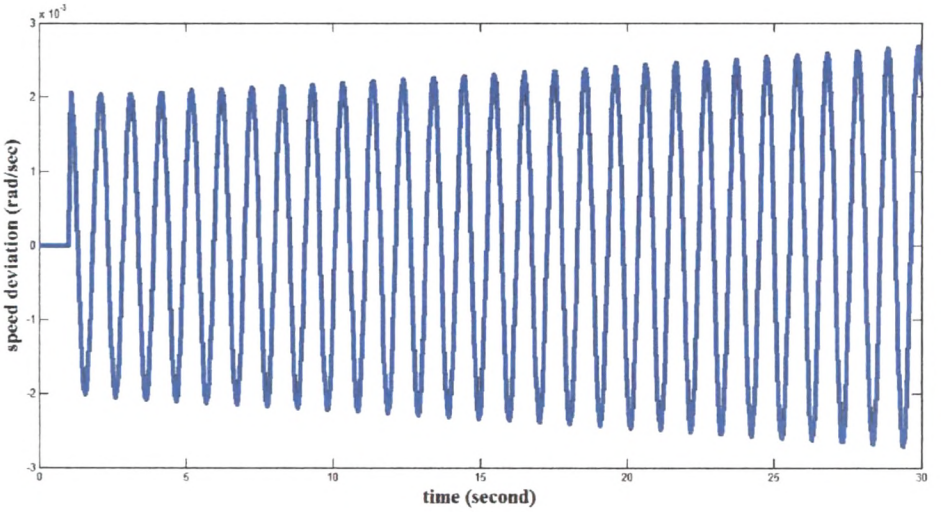

Figure 3.7: Case I : Speed deviation between 0s to 30s with damping coefficient $D = 0$ and without controller (PSS and TCSC)

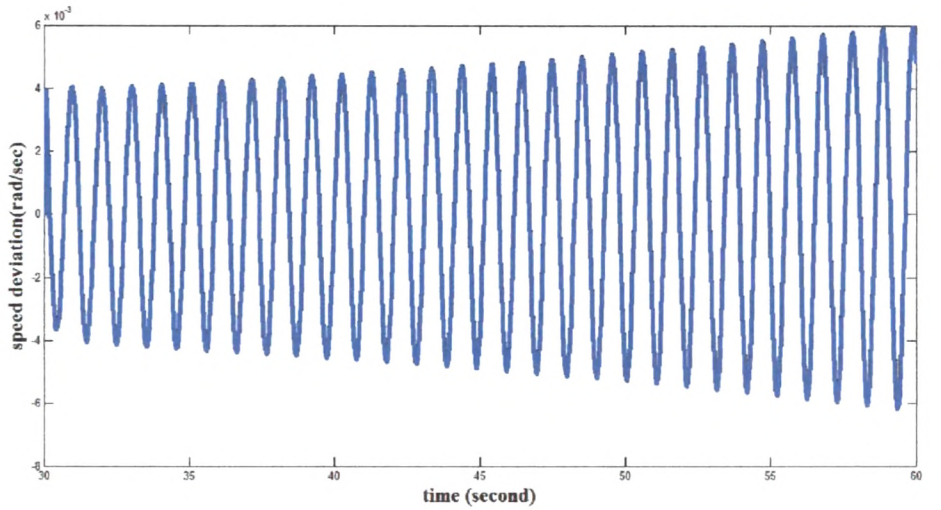

Figure 3.8: Case I : Speed deviation between 30s to 60s with damping coefficient $D = 0$ and without controllers(PSS and TCSC)

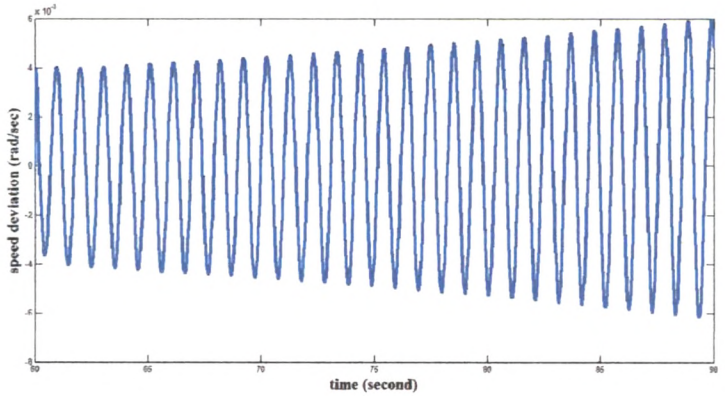

Figure 3.9: Case I : Speed deviation between 60s to 90s with damping coefficient $D = 0$ and without controller (PSS and TCSC)

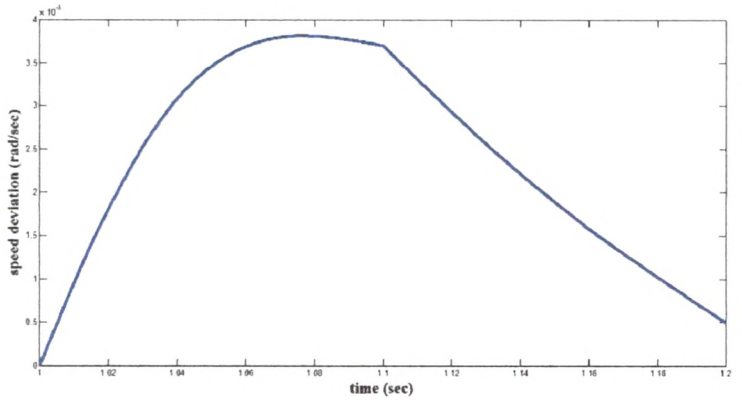

Figure 3.10: Case I : Speed deviation between 1s to 1.2s with zero damping coefficient $D = 0$ and without controller(PSS and TCSC)

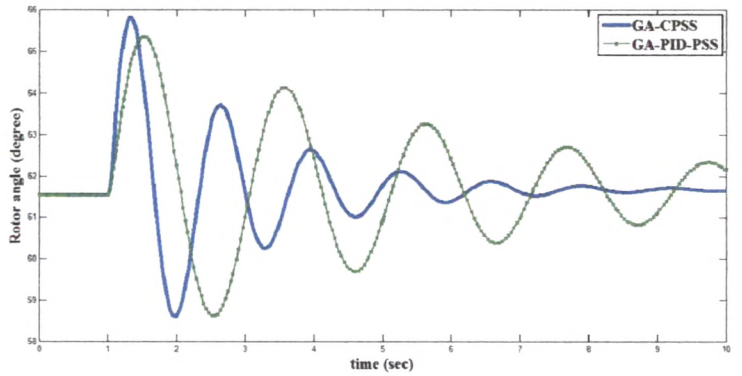

Figure 3.11: Case I: Rotor angle with GA based PSSs

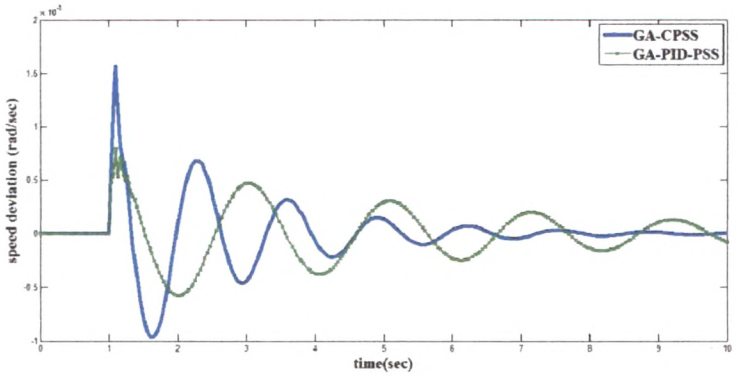

Figure 3.12: Case I: Speed deviation with GA based PSSs

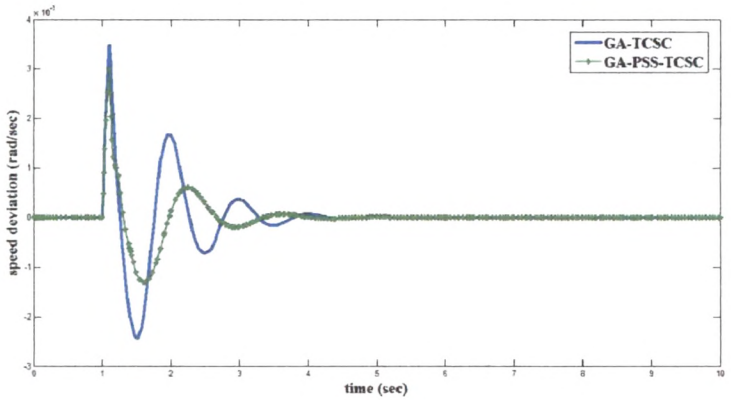

Figure 3.13: Case I: Speed deviation with GA based TCSC and PSS-TCSC

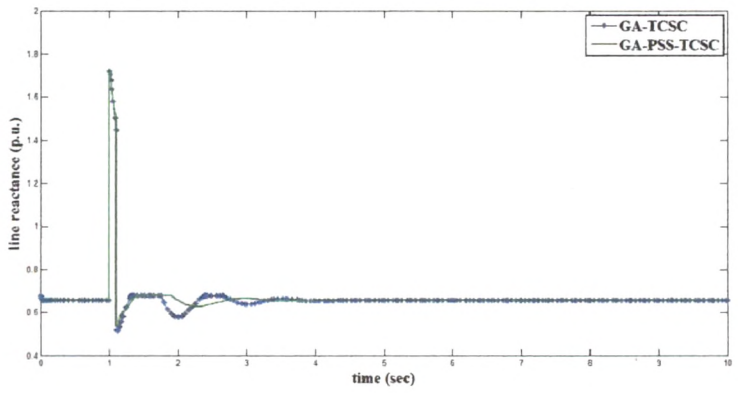

Figure 3.14: Case I: Line reactance with GA based TCSC and PSS-TCSC

3.4.2 Case II

$P_t = 0.6, Q_t = 0.0224$, A three phase fault is created at 1s at the middle of one transmission line and cleared after 50 ms by the disconnection of the faulted line, and then successfully reclosed at 5s [71]. Figure 3.15 shows the response of the rotor speed deviation with damping coefficient $D = 0$ and without PSS and TCSC damping controllers. The response of the δ and ω_m with the presence of GA based CPSS and PID-PSS have been shown in Figure 3.16 and 3.17 respectively. The response of ω_m with individual and simultaneously application of GA based TCSC and PSS has been shown in Figure 3.18. Without application of damping controllers, the oscillations in speed deviation have been observed. These oscillations are continuous growing, which shows instability of system after 10s. While using the individual PSSs and TCSC and simultaneous application of GA based PSS-TCSC significantly diminished this oscillations and improved stability of the system.

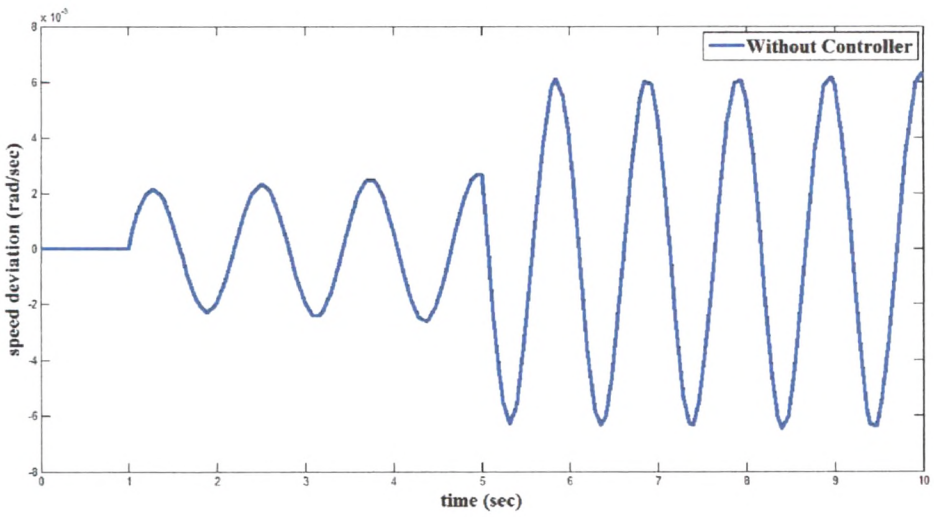

Figure 3.15: Case II: Speed deviation with damping coefficient $D = 0$ and without controller (PSS and TCSC)

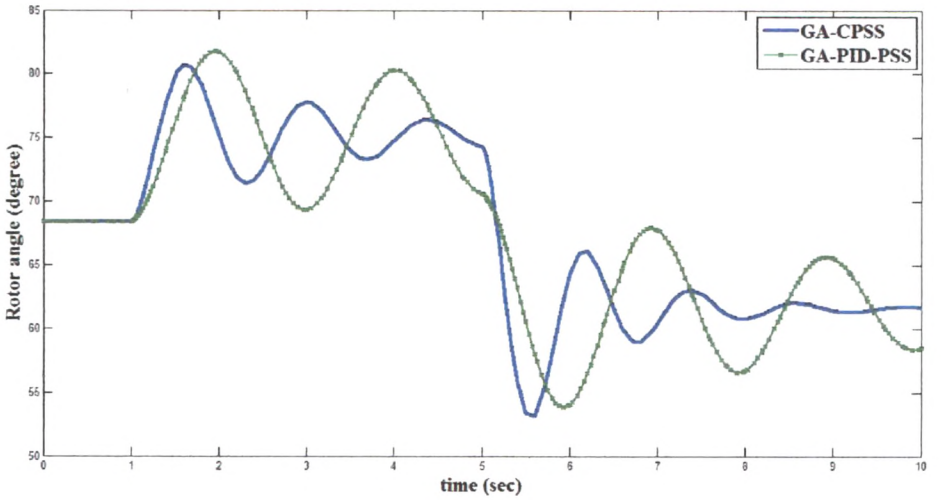

Figure 3.16: Case II: Rotor angle with GA based PSSs

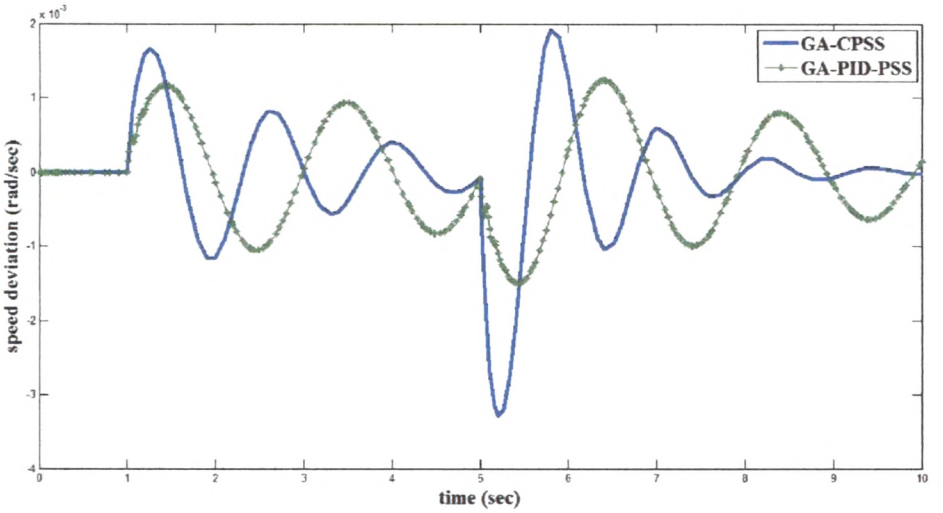

Figure 3.17: Case II: Speed deviation with GA based PSSs

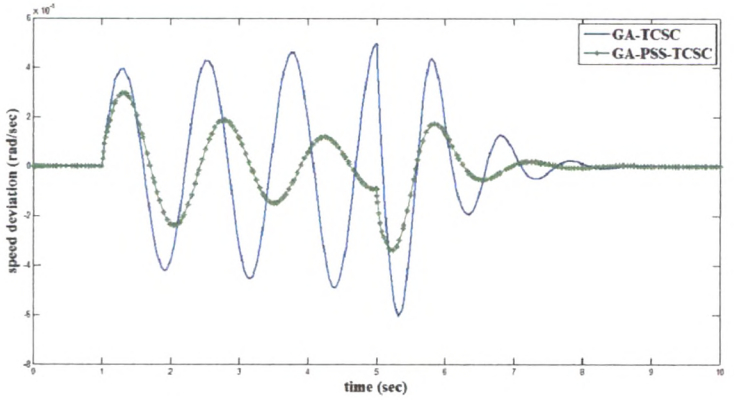

Figure 3.18: Case II: Speed deviation with GA based TCSC and PSS-TCSC

3.4.3 Case III

$P_t = 0.9, Q_t = 0.12$, Here heavy loading condition is considered. A three phase fault is created at 1s at the sending end of one of the circuits of the transmission line and cleared after 50ms. Figures 3.19, 3.20, 3.21 and 3.22 have shown the response of speed deviation between 1s to 1.2s, 1s to 2s, 2s to 7s and 0s to 10s respectively with damping coefficient $D = 0$ and without damping controllers. Under heavy loading condition, the system lost its stability very quickly and system became unstable. Figure 3.23 shows the response of the ω_m with the presence of GA based CPSS and PID-PSS. Figure 3.24 shows the response of ω_m with individual and simultaneous application of GA based TCSC and PSS. While using individual GA based PSSs and TCSC and simultaneous application of GA based PSS-TCSC provided excellent damping characteristics.

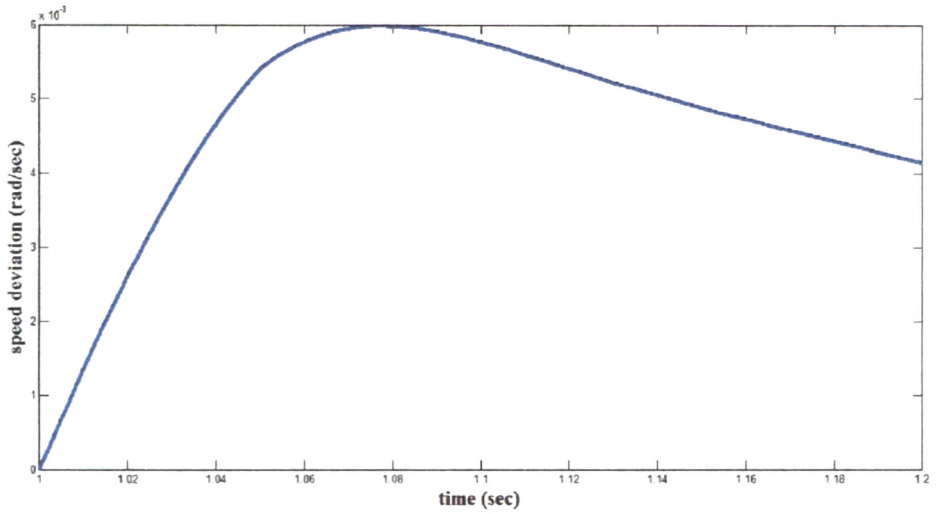

Figure 3.19: Case III : Speed deviation between 1s to 1.2s with damping coefficient $D = 0$ and without controller(PSS and TCSC)

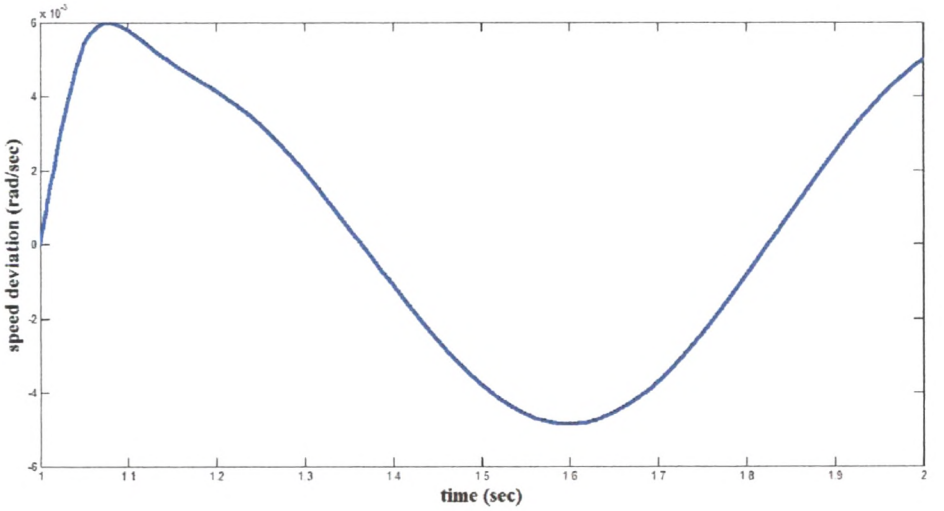

Figure 3.20: Case III : Speed deviation between 1s to 2s with damping coefficient $D = 0$ and without controllers (PSS and TCSC)

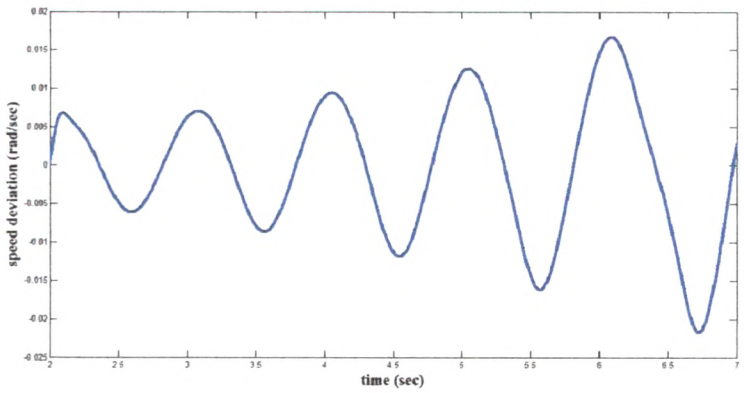

Figure 3.21: Case III : Speed deviation between 2s to 7s with damping coefficient $D = 0$ and without controller(PSS and TCSC)

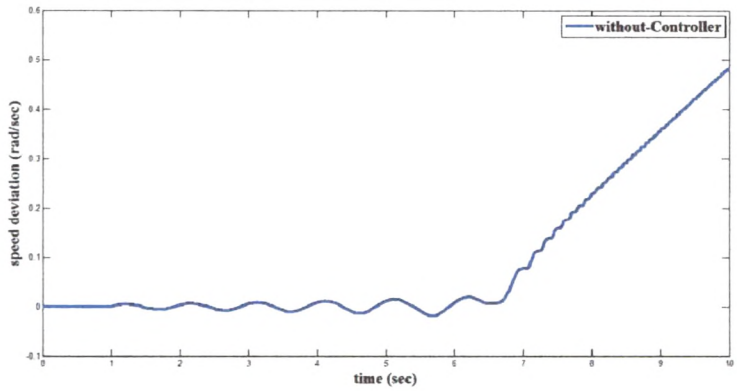

Figure 3.22: Case III: Speed deviation between 0s to 10s with damping coefficient $D = 0$ and without controller (PSS and TCSC)

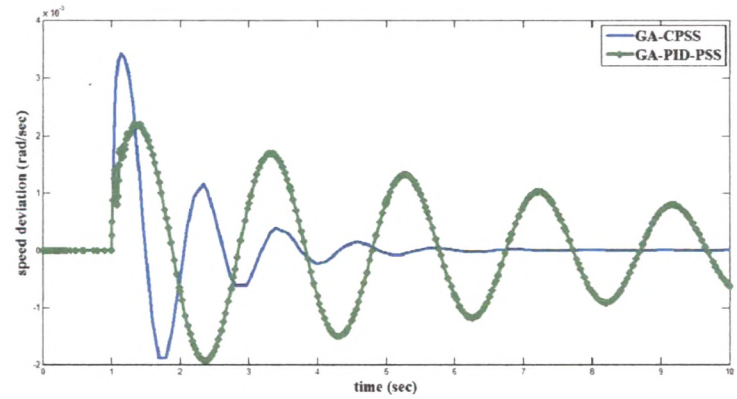

Figure 3.23: Case III: Speed deviation with GA based PSSs

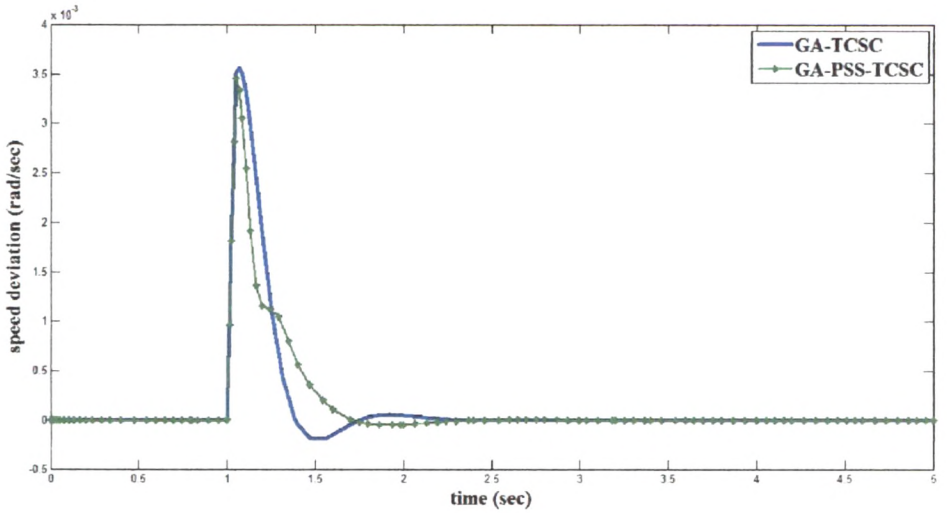

Figure 3.24: Case III: Speed deviation with GA based TCSC and PSS-TCSC

3.4.4 Case IV

$P_t = 0.9, Q_t = 0.12$, Under the heavy loading condition, a 10% mechanical change applied at 1s and removed at 5s is considered. The response of rotor speed deviation between 1s to 4s and 0s to 10s has been shown in Figure 3.25 and Figure 3.26 respectively with damping coefficient $D = 0$ and without application of PSS and TCSC damping controllers. The system lost its stability at 4s which has been shown by Figure 3.26. The response of the ω_m with the presence of GA based CPSS and PID-PSS has been shown in Figure 3.27. The response of ω_m with individual and simultaneously application of GA based TCSC and PSS has been shown in Figure 3.28. Variations in the speed response are observed at 1s and 5s with controllers because mechanical change is applied at same instant. The simultaneous application of PSS and TCSC has been provided very good stability to system compared to individual application of PSS and TCSC.

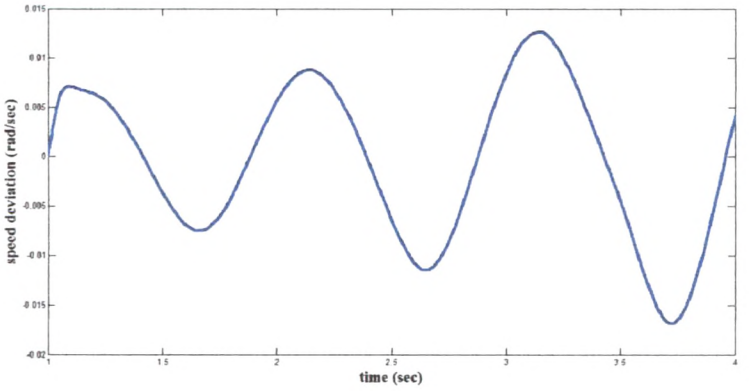

Figure 3.25: Case IV: Speed deviation between 1s to 4s with damping coefficient $D = 0$ and without controller (PSS and TCSC)

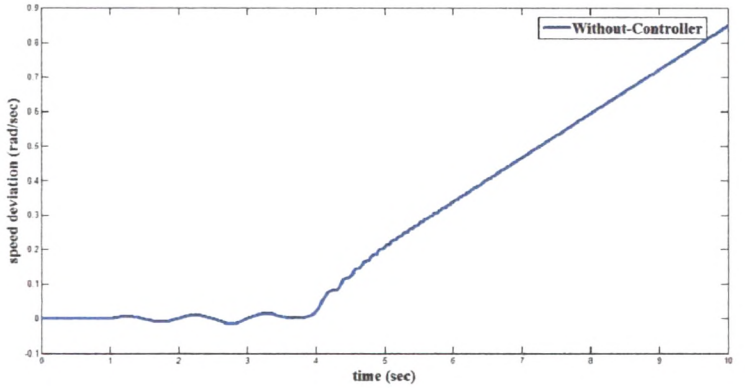

Figure 3.26: Case IV: Speed deviation between 0s to 10s with damping coefficient $D = 0$ and without controller (PSS and TCSC)

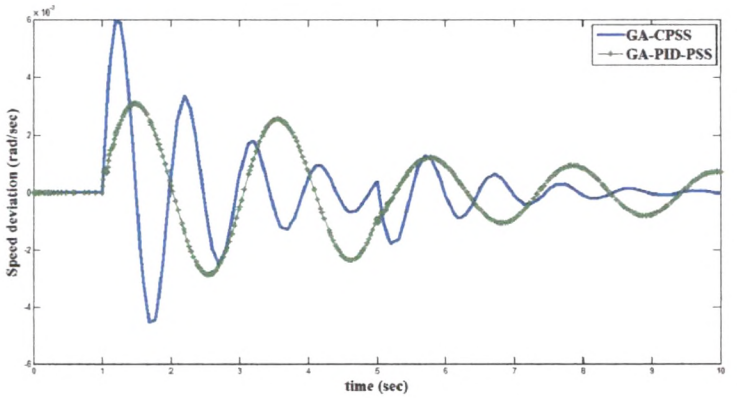

Figure 3.27: Case IV: Speed deviation with GA based PSSs

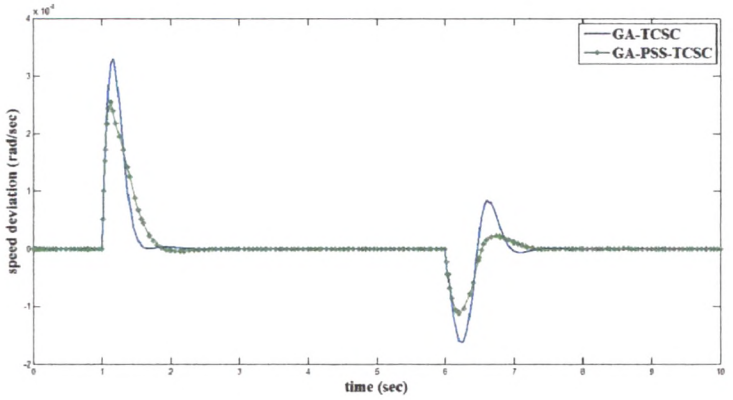

Figure 3.28: Case IV: Speed deviation with GA based TCSC and PSS-TCSC

3.4.5 Case V

$P_t = 1.2, Q_t = 0.2$, Under very heavy loading condition, a 10% input terminal voltage applied at 1s and removed at 5s is considered. The response of the rotor speed deviation with damping coefficient $D = 0$ without controllers has been shown in Figure 3.29 and Figure 3.30. Under heavy loading condition, the system lost its stability very quickly and system became unstable. Figure 3.31 shows the response of the ω_m with the presence of GA based CPSS and PID-PSS. Figure 3.32 shows that the system lost its stability using the individual application of TCSC with continuous growing of oscillation, while simultaneous application of GA based TCSC and PSS provides stability to system.

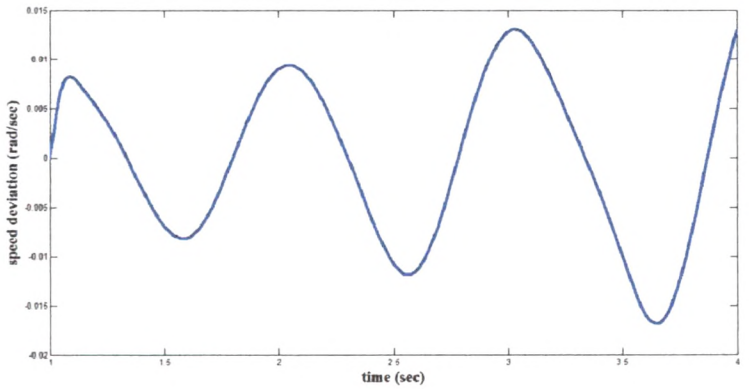

Figure 3.29: Case V: Speed deviation between 1s to 4s with damping coefficient $D = 0$ and without controller (PSS and TCSC)

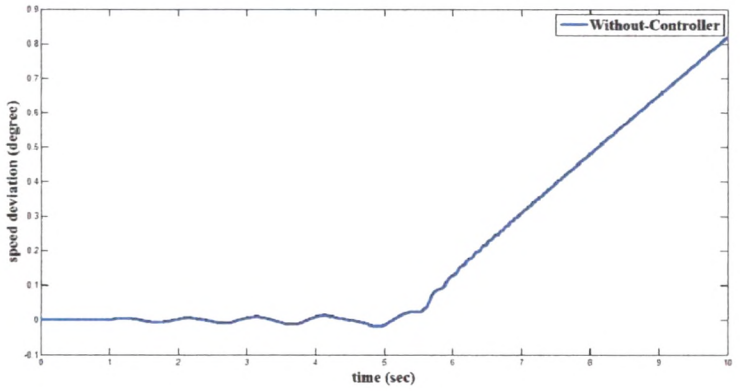

Figure 3.30: Case V: Speed response between 0s to 10s with damping coefficient $D = 0$ and without controller (PSS and TCSC)

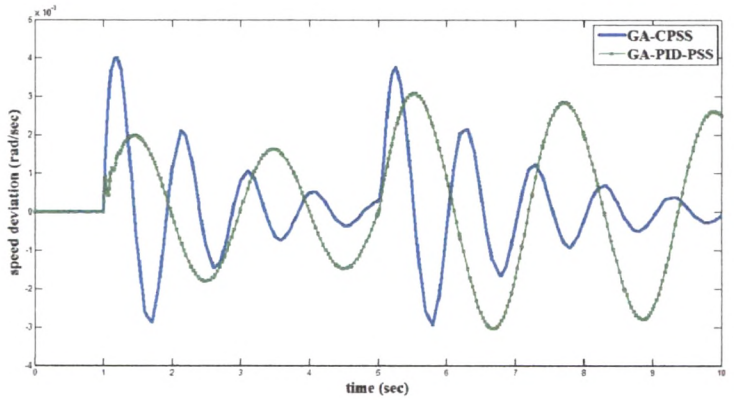

Figure 3.31: Case V: Speed deviation with GA based PSSs

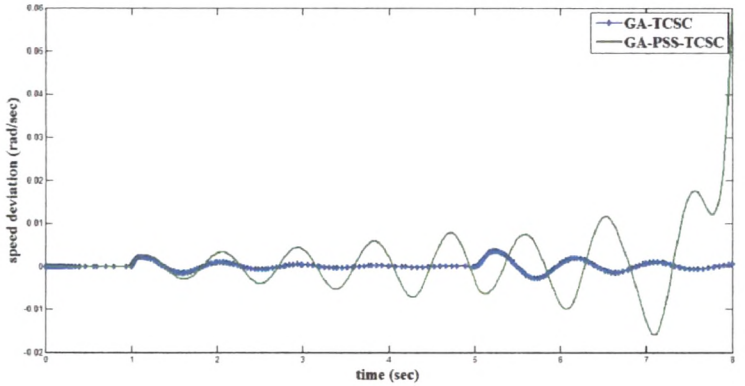

Figure 3.32: Case V: Speed deviation with GA based PSS and PSS-TCSC

3.4.6 Case VI

$P_t = 0.75, Q_t = 0.1$, In this case another severe disturbance is considered. One of the transmission lines is permanently tripped at 1s. The transmission line reactance is suddenly increased and system lost its stability very rapidly. The response of the rotor speed deviation with damping coefficient $D = 0$ and without controllers has been shown in Figure 3.33 and Figure 3.34. The response of the δ and ω_m with the presence of GA based CPSS and PID-PSS have been shown in Figure 3.35 and 3.36 respectively. The response of ω_m with individual and simultaneous application of GA based TCSC and PSS has been shown in Figure 3.37.

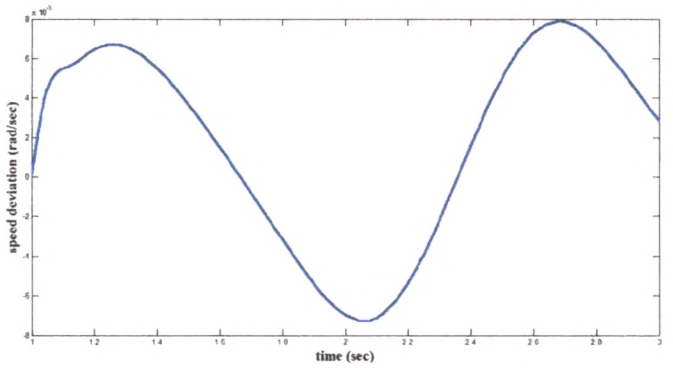

Figure 3.33: Case VI: Speed deviation between 1s to 3s with damping coefficient $D = 0$ and without controller (PSS and TCSC)

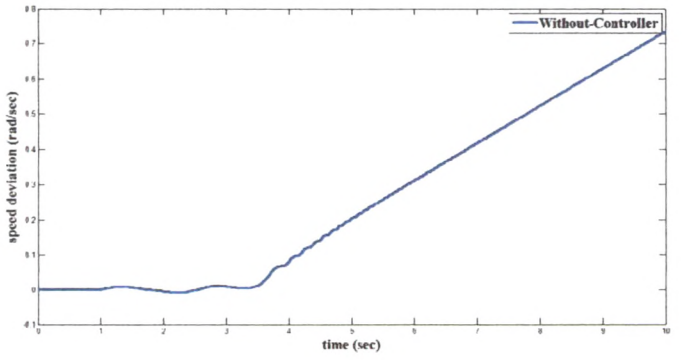

Figure 3.34: Case VI: Speed deviation between 0s to 10s with damping coefficient $D = 0$ and without controller (PSS and TCSC)

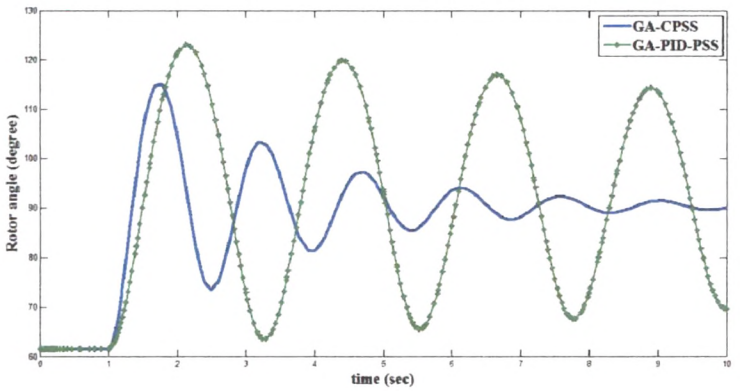

Figure 3.35: Case VI: Rotor angle with GA based PSSs

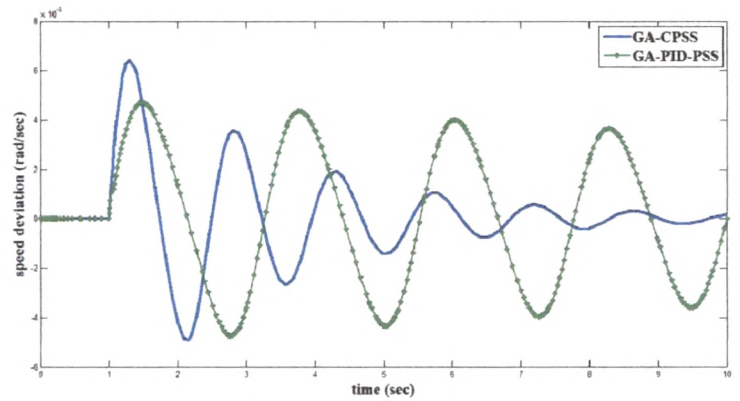

Figure 3.36: Case VI: Speed deviation with GA based PSSs

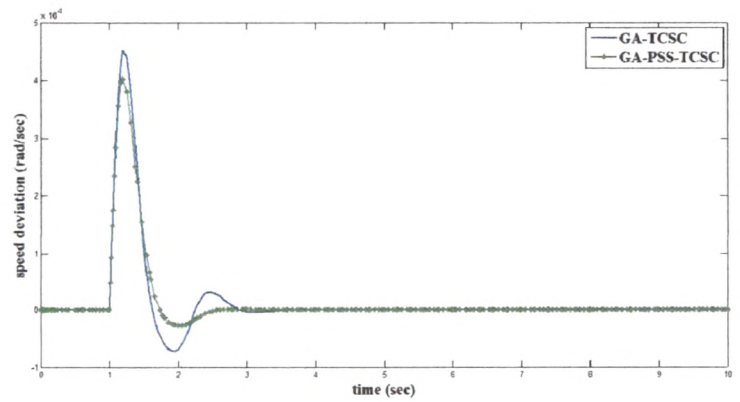

Figure 3.37: Case VI: Speed deviation with GA based PSS and PSS-TCSC

3.5 Conclusion

In this study, Genetic Algorithm based control strategies have been developed for designing of PSSs and TCSC damping controller. The PSSs and simultaneous designed TCSC and PSS have been applied to the dynamical power system. The small signal stability analysis and non-linear simulation for the transient stability analysis have been carried out for detailed investigation of the power system stability issue. Four different operating conditions have been taken and the responses of the rotor angle, rotor speed deviation, terminal voltage and net reactance have been analyzed under different types of the disturbances and faults.

It has been shown that the eigen values associated to the electromechanical mode are more negative with presence of CPSS and PID-PSS in power system and poles in s-plane are far away from origin. The damping factor has been improved with PSSs compare to the without PSSs, which shown that the system is more stable and PSSs have been provided good damping to oscillation in power system. It has been also observed that with the simultaneous application of PSS and TCSC in power system, the eigen values are more negative and damping factor has been improved significantly, which shows good stability of system compare to the individual application of PSS and TCSC.

From the non - linear analysis, without the application of the controllers in the system, the oscillations in rotor angle, rotor speed deviation have been observed. Under the heavy loading conditions, it has been cleared that if the active power and reactive power are increased, the oscillation in rotor angle and speed deviation are continuously growing which creates the instability of the system under the contingencies. The simultaneously designed TCSC and PSS damping controller have been significantly diminished oscillations in system. Simultaneously application of TCSC and PSS have been provided very good damping characteristics compare to the individual application of PSSs or TCSC and almost eliminate the oscillations in system. Application of GA based TCSC and PSSs have improved the time response parameters such as settling time, rise time and delay time appreciably and also decreased the overshoot in the system.